

Acceleration by aerosol of a radiative-thermodynamic cloud feedback influencing Arctic surface warming

Timothy J. Garrett,¹ Melissa M. Maestas,¹ Steven K. Krueger,¹ and Clinton T. Schmidt¹

Received 22 July 2009; revised 3 September 2009; accepted 10 September 2009; published 8 October 2009.

[1] Recent work suggests that short-lived pollutants with mid-latitude origins are contributing to observed warming of the Arctic surface. Candidate mechanisms include an “aerosol indirect effect” associated with increases in cloud longwave emissivity: small cloud droplets associated with polluted conditions are efficient absorbers and emitters of longwave radiation. Here, we argue that the associated surface warming can be temporarily amplified: particulate pollution, by increasing cloud emissivity, additionally accelerates a pre-existing positive feedback loop between cloud top radiative cooling and new droplet condensation. **Citation:** Garrett, T. J., M. M. Maestas, S. K. Krueger, and C. T. Schmidt (2009), Acceleration by aerosol of a radiative-thermodynamic cloud feedback influencing Arctic surface warming, *Geophys. Res. Lett.*, 36, L19804, doi:10.1029/2009GL040195.

1. Introduction

[2] Recent concerns about the high rate of Arctic sea-ice melting have generated a resurgence of interest in the controlling role of clouds in the local surface radiation balance [Francis and Hunter, 2006, 2007; Kay *et al.*, 2008].

[3] Short-lived anthropogenic pollutants from mid-latitudes may also play a contributing role [Quinn *et al.*, 2008]. Arctic aerosols, for example [Shaw, 1982; Quinn *et al.*, 2007], have been shown to be associated with an increase in longwave surface radiative forcing by thin Arctic low-level liquid clouds of several watts per meter squared [Lubin and Vogelmann, 2006; Garrett and Zhao, 2006]. Higher concentrations of aerosol particles make droplets smaller causing instantaneously higher cloud thermal emission [Garrett *et al.*, 2002].

[4] In this paper, we explore whether aerosol can increase cloud thermal emission not only by decreasing the droplet effective radius of clouds, but also through a radiative-thermodynamic feedback loop.

2. Analytical Description

[5] Traditionally, efforts directed at analytical descriptions of the physics of cloud-topped boundary layers have focused not on the Arctic but on more mid-latitude oceanic regions [e.g., Lilly, 1968; Wood, 2007]. Cloud evolution is evaluated by tracking two conserved variables: the total water mass mixing ratio

$$Q = q_v + q_c \quad (1)$$

where, in a cloud q_c is positive and $q_v = q_v^{sat}(T, p)$ – the saturation water vapor mixing ratio at temperature T and pressure p . Also, there is the moist static energy

$$h_m = gz + c_p T + L_v q_v \quad (2)$$

where gz is the geopotential, $c_p T$ is the sensible heat and $L_v q_v$ latent heat. In “mixed-layer model” treatments, it is normally assumed that boundary-layer Q and h_m are independent of height, and determined by surface fluxes, cloud-top turbulent entrainment, and radiative flux divergence.

[6] In the Arctic, however, there is often a strong surface inversion approaching 10°C during winter [Kahl, 1990] and cloud layers are effectively decoupled from surface fluxes of moisture and heat. In this regard, an “elevated mixed-layer” model, as applied previously to altocumulus clouds [Liu and Krueger, 1998] might seem simpler and more appropriate. However, even in the warmer summer months, Arctic boundary layer convection tends to be weak enough that cloud-top turbulent entrainment is also small [Curry, 1986]. Then, to first-order, Arctic stratus evolution might be reduced to a straight-forward thermodynamic response to radiative flux divergence.

[7] What follows is a simplified analytic model for this scenario. As simplifying assumptions, the cloud is treated as a thin, vertically decoupled mixed-layer that is effectively isothermal with temperature T_c and thickness δz and is exposed to the atmosphere above at effective temperature T_a and the surface below at temperature T_s .

[8] Cloud cooling associated with net flux divergence is in proportion to cloud longwave emissivity ε through the Stefan-Boltzmann relation $F_{LW} = \varepsilon \sigma T^4$

$$-\frac{dh_m}{dt} = -\frac{1}{\rho_a} \frac{\partial F_{LW}^{net}}{\partial z} \simeq -\frac{1}{\rho_a} \frac{\varepsilon}{\delta z} \sigma (2T_c^4 - T_s^4 - T_a^4) \quad (3)$$

where, ρ_a is the air density. In the presence of a surface inversion, cooling depresses the saturation mixing ratio of water vapor, forcing condensate production in accordance with the Clausius-Clapeyron relation.

$$\frac{de^{sat}}{dt} = \frac{de^{sat}}{dT} \frac{dT_c}{dt} = \frac{L_v e^{sat}}{(1 + \gamma)c_p R_v T_c^2} \frac{dh_m}{dt} \quad (4)$$

where, R_v is the gas constant for water vapor and $\gamma = L_v/c_p(dq_v^{sat}/dT|_p)$ [Arakawa and Schubert, 1974]. For colder temperatures near 250 K that might be found in a wintertime Arctic stratus layer, $\gamma \sim 0.1$.

[9] Of course, condensate production is also balanced by condensate loss through precipitation at some unknown rate P . Taking this into account, and combining equations (1), (3) and (4), yields the following mass balance for the

¹Department of Atmospheric Sciences, University of Utah, Salt Lake City, Utah, USA.

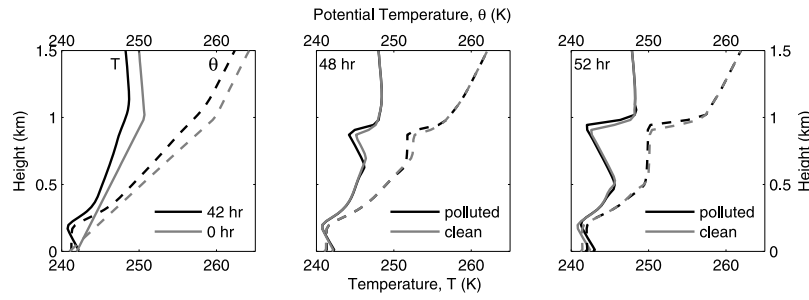


Figure 1. (left) Evolution of the boundary layer profiles in temperature (T , solid) and potential temperature (θ , dashed), starting from initial conditions at 0 hr to initial cloud formation at 42 hr, and profiles for nominally polluted ($r_e = 6 \mu\text{m}$) and clean ($r_e = 12 \mu\text{m}$) conditions at (middle) 48 hr and (right) 52 hr.

logarithmic evolution of condensate concentrations q_c in an isothermal cloud

$$\frac{\partial \ln q_c}{\partial t} = \frac{L_v q_v^{\text{sat}}(T_c)}{\rho_a (1 + \gamma) c_p R_v T_c^2} \frac{\sigma (2T_c^4 - T_s^4 - T_a^4)}{\delta z} \frac{\varepsilon}{q_c} - \frac{P}{q_c} \quad (5)$$

In the long-run, the system moves towards an equilibrium state where either longwave radiative convergence and divergence balance or precipitation balances radiatively-driven condensation.

[10] For the transient condition, however, evolution of condensation is driven by thermal emission through the cloud emissivity ε . Cloud emissivity itself is dependent on the concentration of condensate q_c through the approximate relationship

$$\varepsilon \simeq 1 - \exp(-\beta k(r_e) \rho_a q_c \delta z) \quad (6)$$

The exponent includes the effective radius dependent mass-specific absorption coefficient $k(r_e)$, the density of air ρ_a , and a diffusion coefficient $\beta \simeq 1.7$ [Hermann, 1980; Garrett et al., 2002].

[11] Taking the e-folding depth for absorption of thermal radiation by cloud to be $h = 1/(\beta k(r_e) \rho_a q_c)$, equation (6) provides the following expression for the evolution of ε

$$\frac{\partial \ln \varepsilon}{\partial t} = \frac{\delta z}{h} \frac{(1 - \varepsilon)}{\varepsilon} \frac{\partial \ln q_c}{\partial t} \quad (7)$$

[12] Equations (5) and (7) represent a positive feedback loop for the evolution of cloud. Cloud thermal emission drives condensation through radiative cooling (equation (5)). In return, condensation corresponds to higher efficiency of thermal emission (equation (7)) [see also Randall and Suarez, 1984]. Put simply, cloud begets more cloud. Of course, the rate of return for this feedback loop diminishes as the cloud and surface temperatures equilibrate or as the cloud approaches a thermal blackbody and $\varepsilon \simeq 1$.

[13] The added subtlety that we introduce is to suggest that pollution, by making droplets smaller, increases the value of the mass-specific absorptivity $k(r_e)$ [Garrett et al., 2002], decreasing the cloud thermal absorption depth h , thereby accelerating radiative flux divergence through $\partial \ln \varepsilon / \partial t$ (equation (7)). What this means is that, all other things being equal, the aforementioned feedback loop between condensate production and radiative cooling becomes more

efficient. Not only does cloud beget more cloud, but if it is polluted, it is more fecund.

3. Numerical Simulations

3.1. Numerical Setup

[14] To test the above hypothesis, we have performed numerical simulations using the University of Utah Large Eddy Simulation Model (UU LESM) [Zulauf, 2001]. The UU LESM is specifically designed for examination of small-scale, short period atmospheric flows, particularly those involving cloud-scale processes such as convection, entrainment, and turbulence. The dynamic framework is based upon the 3D nonhydrostatic primitive equations. Rather than using an anelastic set of governing equations, the quasi-compressible approximation is used [Droegemeier and Wilhelmson, 1987], in which the speed of sound is artificially reduced. The code includes interactive radiative transfer [Fu et al., 1995] and has been used to study aspects of a wide range of cloud systems, including cumulus convection, deep convection, and anvil cirrus.

[15] Here, simulations employ a periodic model domain that is $2040 \text{ m} \times 3060 \text{ m}$ in horizontal extent. Although calculations extend through a full atmospheric profile, a sponge layer is implemented above 3 km to damp atmospheric motions at levels above those of interest. The spatial resolution was chosen to resolve the expected skin depth h of thermal interactions with cloud. In the horizontal domain, the grid size was set to be 30 m, and in the vertical, a stretched grid was employed with a minimum spacing of 25 m in the center of the cloud domain. The model time step was 1.0 s for dynamics and 60 s for radiation, and all model simulations extended for 60 hours. Because simulations are intended to apply to the Arctic night, only thermal radiation was considered.

[16] There was no net subsidence across the domain, and background turbulence was maintained by a horizontal wind speed of 10 m s^{-1} . The model was initialized with a standard winter Arctic temperature and trace greenhouse gas profiles characterized by a surface temperature of $-31.2 \text{ }^\circ\text{C}$ with a $10 \text{ }^\circ\text{C}$ temperature inversion extending up to 1 km altitude [Key and Schweiger, 1998] (Figure 1). The humidity profiles were initialized such that below 1 km altitude, the relative humidity with respect to water was 80% and above this level the relative humidity with respect to ice was 50%. The intent here was to create a boundary layer sufficiently opaque in the infrared that, with time, it

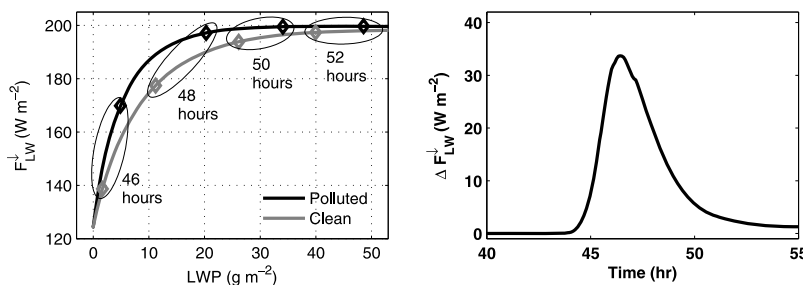


Figure 2. (left) Phase diagram showing the evolution of domain-averaged downwelling surface longwave radiation F_{LW}^{\downarrow} and liquid water path LWP under nominally polluted ($r_e = 6 \mu m$) and nominally clean ($r_e = 12 \mu m$) conditions, for cases where surface temperature was allowed to instantaneously adjust. Ovals connect points with the same evolutionary time. (right) Evolution of the difference between polluted and clean F_{LW}^{\downarrow} .

would spontaneously nucleate cloud through clear-sky radiative cooling. Thus, cloud is not prescribed in these simulations, but allowed to form naturally as a plausible consequence of prior exposure to a moisture source, such as sea ice leads or horizontal advection.

3.2. Experimental Setup and Results

[17] Model microphysics was set to be purposefully simple, accounting only for liquid condensation and evaporation through a “saturation adjustment scheme” [Lord *et al.*, 1984; Krueger *et al.*, 1995]. No account was made for precipitation formation (i.e. $P = 0$), or droplet settling [Ackerman *et al.*, 2009]. Droplet size was simply specified so that a fixed droplet effective radius r_e of $6 \mu m$ plausibly represented nominally polluted cloud runs, and a value of $12 \mu m$ to nominally clean cloud runs. In every other regard the polluted and clean runs were identical. The advantage of this approach is that it permits straight-forward isolation of hypothesized radiative-thermodynamic feedbacks from their potentially complicated interactions with additional processes.

[18] Two additional cases were also considered. In the first case, surface temperature was held fixed. In reality, the snow-covered surface rapidly equilibrates to the effective radiative temperature of the cloudy atmosphere above [Sverdrup, 1933; Persson *et al.*, 2002]. As implied by equation (5), if T_s and T_c are allowed to equilibrate to each other, flux divergence is smaller and condensation slowed. Thus, a second case allowed for instantaneous surface

temperature adjustment to warmer atmospheric radiative temperatures. The real sensitivity of Arctic cloud should be bounded by these two extreme scenarios.

[19] As shown in Figure 1, the clear-sky boundary-layer cooled radiatively. After nearly 2 days model simulation time, cloud formed near boundary-layer top where it created a progressively deepening mixed-layer through a positive feedback loop relating condensation to cloud thermal emission (equations (5) and (7)). A mixed-layer also developed at the surface, but the cloud and surface remained decoupled throughout the simulation.

[20] Figure 2 shows that as cloud liquid water path LWP developed, surface downwelling longwave fluxes F_{LW}^{\downarrow} grew rapidly, up to the point that cloud thermal emission saturated when LWP exceeded about $40 g m^{-2}$. If surface temperature was not allowed to adjust in the model (not shown), simulated values of F_{LW}^{\downarrow} differed negligibly, the solution diverging by less than $1 W m^{-2}$ by the time step of 55 hours.

[21] What Figures 2 and 3 indicate is that cloud development is accelerated under nominally polluted conditions. Clouds with $6 \mu m$ droplets have a value of h in equation (7) that is approximately 30% smaller than clouds with $12 \mu m$ droplets [Garrett *et al.*, 2002]. Through coupling with equation (5), the formation of condensate is more rapid, and, at a given time, downwelling longwave radiation at the surface is substantially higher, by up to $36 W m^{-2}$. A positive difference is maintained for a period of approximately 10 hours until saturation of thermal emission.

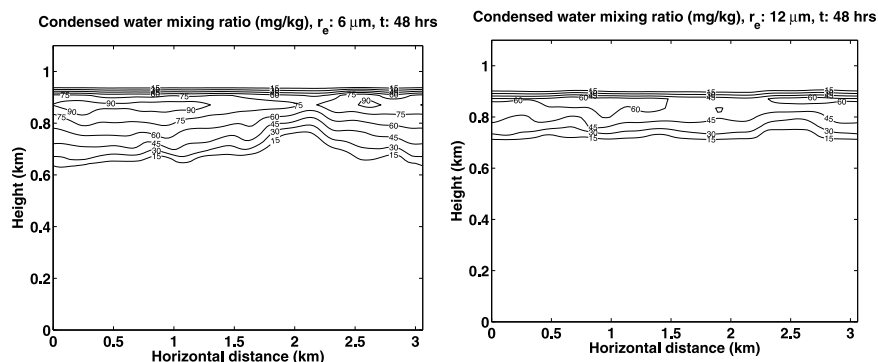


Figure 3. For the case with surface-temperature adjustment, a comparison of a vertical cross-section through the simulated cloud under (left) nominally polluted ($r_e = 6 \mu m$) and (right) nominally clean ($r_e = 12 \mu m$) conditions after 48 hours model simulation time.

Nominally polluted conditions are associated with a total added energetic input of approximately 0.4 MJ m^{-2} , which, neglecting heat transport in the snow-pack, is sufficient to produce a melt-layer 2 mm deep.

3.3. Summary

[22] Prior work on interactions between industrial pollution and Arctic clouds has focused on an instantaneous magnification of low-level cloud surface heating due to higher cloud emissivity associated with smaller droplets, as might be expected if soluble aerosol loadings are high. Here, we have presented idealized theoretical arguments and numerical simulations that indicate that cloud thermal emission drives a positive feedback loop between rates of condensation and cloud radiative flux divergence. In polluted conditions with smaller cloud droplets the efficiency of the feedback loop is accelerated. Compared to clean clouds, polluted clouds emit an added pulse of atmospheric energy into the Arctic ice sheet. While individual pulses last only hours, the accumulated effect of repeated polluted cloud episodes over a season would represent a substantial anthropogenic contribution to the sea-ice energy balance.

[23] The ultimate contribution of the described sensitivity to the Arctic will require consideration of the response time and magnitude of associated negative feedbacks. While we neglected precipitation in order to focus on sensitivities related to the production side of equation (5), precipitation is a sink for condensation [Harrington *et al.*, 1999; Morrison and Pinto, 2006; Fridlind *et al.*, 2007; Ackerman *et al.*, 2009]. Also, any local perturbation to Arctic energetics might be associated with compensating adjustments in horizontal heat transport from mid-latitudes [Beesley, 2000]. Teasing “cause-and-effect” from a system governed by feedback processes will require an a priori statement of the time-scales of interest.

[24] **Acknowledgments.** This study was initiated by the Clean Air Task Force, with additional support from NSF award ATM0649570, NOAA award NA040AR4310087, and NASA New Investigator Program award NNX06AE24G.

References

- Ackerman, A., *et al.* (2009), Large-eddy simulations of a drizzling, stratocumulus-topped marine boundary layer, *Mon. Weather Rev.*, *137*, 1083–1110, doi:10.1175/2008MWR2582.1.
- Arakawa, A., and W. H. Schubert (1974), Interaction of a cumulus cloud ensemble with the large-scale environment, part I, *J. Atmos. Sci.*, *31*, 674–701.
- Beesley, J. A. (2000), Estimating the effect of clouds on the Arctic surface energy budget, *J. Geophys. Res.*, *105*(D8), 10,103–10,117, doi:10.1029/2000JD900043.
- Curry, J. (1986), Interactions among turbulence, radiation and microphysics in Arctic stratus clouds, *J. Atmos. Sci.*, *43*, 90–106.
- Droegemeier, K. K., and R. B. Wilhelmson (1987), Numerical simulation of thunderstorm outflow dynamics. Part I: Outflow sensitivity experiments and turbulence dynamics, *J. Atmos. Sci.*, *44*, 1180–1210.
- Francis, J. A., and E. Hunter (2006), New insight into the disappearing Arctic sea ice, *Eos Trans. AGU*, *87*, 509, doi:10.1029/2006EO460001.
- Francis, J. A., and E. Hunter (2007), Changes in the fabric of the Arctic’s greenhouse blanket, *Environ. Res. Lett.*, *2*(4), 045011, doi:10.1088/1748-9326/2/4/045011.
- Fridlind, A. M., A. S. Ackerman, G. McFarquhar, G. Zhang, M. R. Poellot, P. J. DeMott, A. J. Prenni, and A. J. Heymsfield (2007), Ice properties of single-layer stratocumulus during the Mixed-Phase Arctic Cloud Experiment: 2. Model results, *J. Geophys. Res.*, *112*, D24202, doi:10.1029/2007JD008646.
- Fu, Q., S. K. Krueger, and K.-N. Liou (1995), Interactions of radiation and convection in simulated tropical cloud clusters, *J. Atmos. Sci.*, *52*, 1310–1328.
- Garrett, T. J., and C. Zhao (2006), Increased Arctic cloud longwave emissivity associated with pollution from mid-latitudes, *Nature*, *440*, 787–789, doi:10.1038/nature04636.
- Garrett, T. J., L. F. Radke, and P. V. Hobbs (2002), Aerosol effects on the cloud emissivity and surface longwave heating in the Arctic, *J. Atmos. Sci.*, *59*, 769–778.
- Harrington, J. Y., T. Reisin, W. R. Cotton, and S. M. Kreidenweis (1999), Cloud resolving simulations of Arctic stratus: Part II: Transition-season clouds, *Atmos. Res.*, *51*, 45–75, doi:10.1016/S0169-8095(98)00098-2.
- Hermann, G. F. (1980), Thermal radiation in Arctic stratus clouds, *Q. J. R. Meteorol. Soc.*, *106*, 771–780.
- Kahl, J. D. (1990), Characteristics of the low-level temperature inversion along the Alaskan Arctic coast, *Int. J. Climatol.*, *10*, 537–548.
- Kay, J. E., T. L’Ecuyer, A. Gettelman, G. Stephens, and C. O’Dell (2008), The contribution of cloud and radiation anomalies to the 2007 Arctic sea ice extent minimum, *Geophys. Res. Lett.*, *35*, L08503, doi:10.1029/2008GL033451.
- Key, J., and A. J. Schweiger (1998), Tools for atmospheric radiative transfer: Streamer and Fluxnet, *Comput. Geosci.*, *24*, 443–451.
- Krueger, S. K., Q. Fu, K.-N. Liou, and H.-N. S. Chin (1995), Improvements of an ice-phase microphysics parameterization for use in numerical simulations of tropical convection, *J. Appl. Meteorol.*, *34*, 281–287.
- Lilly, D. K. (1968), Models of cloud-topped mixed layers under a strong inversion, *Q. J. R. Meteorol. Soc.*, *94*, 292–309.
- Liu, S., and S. K. Krueger (1998), Numerical simulations of altocumulus using a cloud resolving model and a mixed layer model, *Atmos. Res.*, *47–48*, 461–474, doi:10.1016/S0169-8095(98)00034-9.
- Lord, S. J., H. E. Willoughby, and J. M. Piotrowicz (1984), Role of a parameterized ice-phase microphysics in an axisymmetric, non-hydrostatic tropical cyclone model, *J. Atmos. Sci.*, *41*, 2836–2848.
- Lubin, D., and A. M. Vogelmann (2006), A climatologically significant aerosol longwave indirect effect in the Arctic, *Nature*, *439*, 453–456, doi:10.1038/nature04449.
- Morrison, H., and J. O. Pinto (2006), Intercomparison of bulk cloud microphysics schemes in mesoscale simulations of springtime Arctic mixed-phase stratiform clouds, *Mon. Weather Rev.*, *134*, 1880–1900, doi:10.1175/MWR3154.1.
- Persson, P. O. G., C. W. Fairall, E. L. Andreas, P. S. Guest, and D. K. Perovich (2002), Measurements near the Atmospheric Surface Flux Group tower at SHEBA: Near-surface conditions and surface energy budget, *J. Geophys. Res.*, *107*(C10), 8045, doi:10.1029/2000JC000705.
- Quinn, P. K., G. Shaw, E. Andrews, E. G. Dutton, T. Ruoho-Airola, and S. L. Gong (2007), Arctic haze: Current trends and knowledge gaps, *Tellus, Ser. B*, *59*, 99–114, doi:10.1111/j.1600-0889.2006.00238.x.
- Quinn, P. K., *et al.* (2008), Short-lived pollutants in the Arctic: Their climate impact and possible mitigation strategies, *Atmos. Chem. Phys.*, *8*, 1723–1735.
- Randall, D. A., and M. J. Suarez (1984), On the dynamics of stratocumulus formation and dissipation, *J. Atmos. Sci.*, *41*, 3052–3057.
- Shaw, G. E. (1982), Evidence for a central Eurasian source area of Arctic haze in Alaska, *Nature*, *299*, 815–818.
- Sverdrup, H. U. (1933), *The Norwegian North Polar Expedition with the “Maud” 1918–1925, Scientific Results*, vol. 2, *Meteorology*, Geofys. Inst., Bergen, Norway.
- Wood, R. (2007), Cancellation of aerosol indirect effects in marine stratocumulus through cloud thinning, *J. Atmos. Sci.*, *64*, 2657–2669, doi:10.1175/JAS3942.1.
- Zulauf, M. A. (2001), Modeling the effects of boundary layer circulations generated by cumulus convection and leads on large-scale surface fluxes, Ph.D. thesis, Univ. of Utah, Salt Lake City.

T. J. Garrett, S. K. Krueger, M. M. Maestas, and C. T. Schmidt, Department of Atmospheric Sciences, University of Utah, 135 South 1460 E, Room 819, Salt Lake City, UT 84112, USA. (tim.garrett@utah.edu)